Int. J. Electrochem. Sci., 8 **(2013)** 3564 - 3571

International Journal of
ELECTROCHEMICAL
SCIENCE
www.electrochemsci.org

Short Communication

Formation of Nanoporous Silver by Dealloying $Ag_{22}Zn_{78}$ Alloy at Low Temperature in H_2SO_4

Zhiqiang Li, Xing Lu[*]*, Zuoxiang Qin*

Liaoning Key Materials Laboratory for Railway, School of Materials Science and Engineering, Dalian Jiaotong University, Dalian 116028, China
[*]E-mail: Luxing64@163.com

Received: 9 January 2013 / *Accepted:* 12 February 2013 / *Published:* 1 March 2013

In this paper, Ag-Zn alloy are dealloyed in 0.1M H_2SO_4 at a low temperature (2°C) to fabricate nanoporous silver and the dealloying kinetics has been systematically investigated. Comparison of the polarization curve of Ag-Zn alloy in 0.1M H_2SO_4 at room temperature and 2°C shows that lowering temperature can significantly reduce the diffusivity of silver atoms and result in forming more exiguous nanoporous silver. SEM observation demonstrates that pores have formed on initial of the dealloying process. The succeeding process just coarsenes pores by silver atoms diffusion and aggregation at the silver/electrolyte interface due to the structure is on a instability state in thermodynamics in the electrolyte. Pore size can grow from tens of nanometers to hundreds of nanometers with the extension of dealloying time in the electrolyte without else treatment. The coarsening exponent and surface diffusivity of silver atoms are estimated to be 4.19 and 1.2×10^{-16} m^2/s. There also exists phase transition in the dealloying process. The forming mechanism of nanoporous silver at low temperature is discussed in the end.

Keywords: Dealloying; Nanoporous silver; Low temperature; Surface diffusivity

1. INTRODUCTION

Nanoporous materials are attracting more and more attentions due to potential technological applications including sensors, micro-actuators, fuel cells and catalysts[1-4]. Nanoporous metals can be fabricated by the template and dealloying approaches. Templating technique fabricates nanoporous materials through replication of porous alumina or liquid-crystal templates. The advantages are precise controlling over the pore size and microstructure periodicity, but normally result in materials with one-

dimensional porosity, such as an array of tubes. It is virtually impossible to dynamic control of the length scale. Dealloying approach is defined as a selective dissolution process, during which the less noble atoms are dissolved from a precursor or alloy, leaving behind a nano-scale, interconnected network of ligaments and open pores. We can flexibly control pore size and its distribution through altering the composition of the precursor or the corrosion parameter, which makes it more popular than the template approach. It has been used in numerous alloy systems, contains Al-Cu[5]、Ag-Au[6-12]、Mn-Cu[13]、Sn-Au[14]、Sn-Ag[15]、Cu-Pt [16]、Zn-Ag[17,18], Al-Ag[19] *etc*.

The ultrafine structure is extraordinary importance in many engineering applications. For example, porous structure anodes can accelerate the anode reaction kinetics due to their high surface areas and nanoporous gold (NPG) with a pore/ligament size of less than 6 nm shows excellent catalytic activity towards CO oxidation at low temperature[20]. The characteristic property of dealloyed materials is the tendency of the nano-scale structure to coarsen with time, increasing the ligament size and spacing and the coarsening mechanism is accepted to be surface diffusion of the remaining noble element, which commences while the removal of the active element is still in progress. The rate of coarsening can be alternated by the addition of surfactants to the electrolyte[21] or dealloyed at a low temperature[22] or incorporation Pt/Pd (very stable, low diffusivity) into the precursor[23], which means dealloying technology can be used in ternary or multiple alloy system to fabricate porous materials with high specific surface area.

Nanoporous silver could be served as the catalyst in the chemical industry such as production of formaldehyde, aldehyde and acetone. It also can be utilized in molecular adsorption, ion exchange, surface-enhanced Raman scattering (SERS), electrochemical sensors [24,25] *etc*. Owing to the fast surface diffusivity, it is hard to fabricate nanoporous silver by dealloying at room temperature (the pore size is about 100-200nm). The current paper describes a simple and effective way via reducing diffusivity to fabricate finer nanoporous silver at a low temperature. The forming process, i.e. the pore size and component *vs* time is addressed. The coarsening exponent and the surface diffusivity are also calculated.

2. EXPERIMENTAL

The Ag-Zn alloy with a nominal composition of 22 at.% Ag was prepared by induction melting pure Ag(99.99 wt.%) and Zn(99.99 wt.%) in the graphite crucible with argon shield, and then the melt was cooled down into ingot in situ. The obtained ingot was annealed at 550 °C for a week and was cut into sheets with a thickness of 2 mm. Then sheets were masked by epoxy resin and the exposed end was ground and polished up to 1 μm diamond.

The electrochemical experiment was performed at 2 °C in 0.1M H_2SO_4 solution by LK98BII electrochemical analyzer. The working electrode、assistant electrode and reference electrode were the alloy、Pt electrode and saturated KCl calomel electrode, respectively. The applied potential is relative

to the saturated KCl calomel electrode potential (SCE). Microstructure characterization and analysis of the alloy and as-dealloyed sample were made using X-ray diffraction(XRD, Empyrean) with Cu Kα radiation, scanning electron microscopy (SEM, JSM 6360LV) with an energy dispersive X-ray (EDX) spectroscopy. The average pore size, defined by the equivalent diameter of pore in nanoporous silver, was determined manually by identifying a minimum of 50 pores, making measurements across the shortest distance of each pore and then averaging. All of the measurement operations were completed by software *Smile view*.

3. RESULTS AND DISCUSSION

The dealloying process is controlled by surface diffusion of the noble element along the alloy/electrolyte interface[26], a low dealloying temperature can effectively reduce the diffusivity of the noble element and delay the coarsening of the nanoporous structure[22], which means lowering the silver diffusivity through controlling temperature can result in a decreasing in size scale of porosity. Figure 1 shows the electrochemical behavior of $Ag_{22}Zn_{78}$ alloy 0.1M H_2SO_4 solution at room temperature(25°C) and 2°C, which was tested through linear sweep voltammetry (LSV). When the electrolyte solution falls from room temperature (25°C) down to 2°C, the corrosion current density minishes dramatically, only about half of the former. From table 1, both the critical potential and self-corrosion potential increase obviously, indicating that lowing temperature can significantly lower the surface diffusivity of silver atoms.

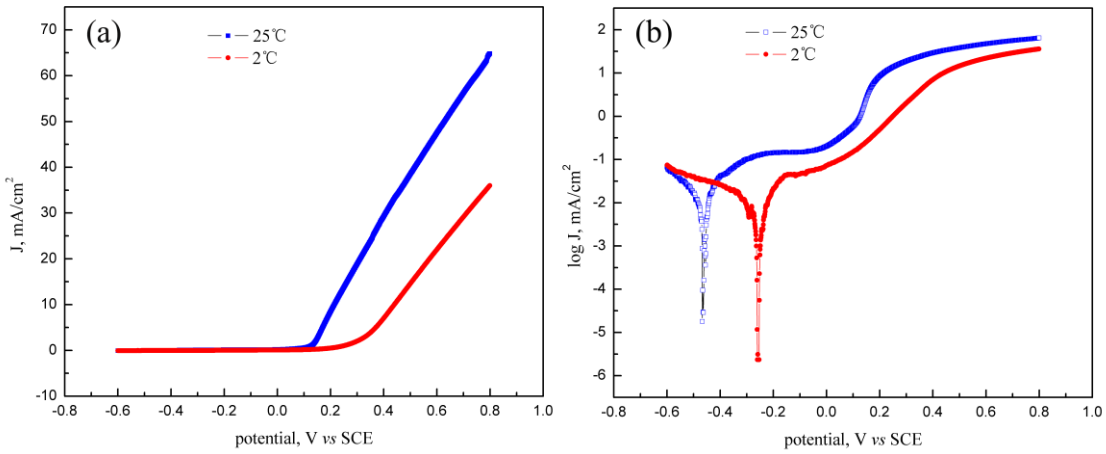

Figure 1. Polarization curve of $Ag_{22}Zn_{78}$ alloy in 0.1M H_2SO_4 at room temperature(25°C) and 2°C, Scan rate 2 mV/s. (a) Variation of current density with potential, which shows a high critical potential at low temperature (b) Tafel polarization curve shows a high self-corrosion potential at low temperature.

Table 1. The self-corrosion potential and critical potential (V, SCE)of $Ag_{22}Zn_{78}$ alloy in 0.1M H_2SO_4 at room temperature(25°C) and 2°C, Scan rate 2 mV/s.

T(°C)	Vself(V, SCE)	Vcrit(V, SCE)
25	-0.46	0.13
2	-0.26	0.25

Figure 2 shows the morphology of nanoporous silver by dealloying $Ag_{22}Zn_{78}$ in 0.1 M H_2SO_4 at temperature of 2°C, which exhibits a uniform, bi-continuous interpenetrating pore/ligament structure. The pore size and ligament width grows with increasing the dealloying time. The pores have formed after one minute's dealloying and the size scale is about 38 nm. For most of the dealloying systems, it is difficult to measure the initial pore/ligament size created during the dealloying process since the nanoporous structure is unstable even at room temperature and undergoes rapid coarsening[27].

It is generally recognized that the dealloying process involves the dissolution of the less noble element and the formation/coarsening of the nanoporous structure by surface diffusion of the more noble element. Theoretical estimates based on percolation length effects in alloy dissolution suggested the pore size should be smaller than 2 nm during the initial stages of the dealloying process[28]. This indicates that the pores/ligaments in the present nanoporous silver undergo significant coarsening during dealloying. In other words, it means that the pore size has formed in the initial moment. In the following dealloying process, the pore size grows up to 52 nm, 62 nm, 81 nm, 94 nm and 112 nm, respectively, which indicates the dealloying time effects on the morphology evidently. The pore coarsenes with time increasing after forming, however, size scale decreases by 30 percent compare to our previous works [28], which shows that low temperature can inhibit silver atoms diffusivity to fabricate finer porous structure.

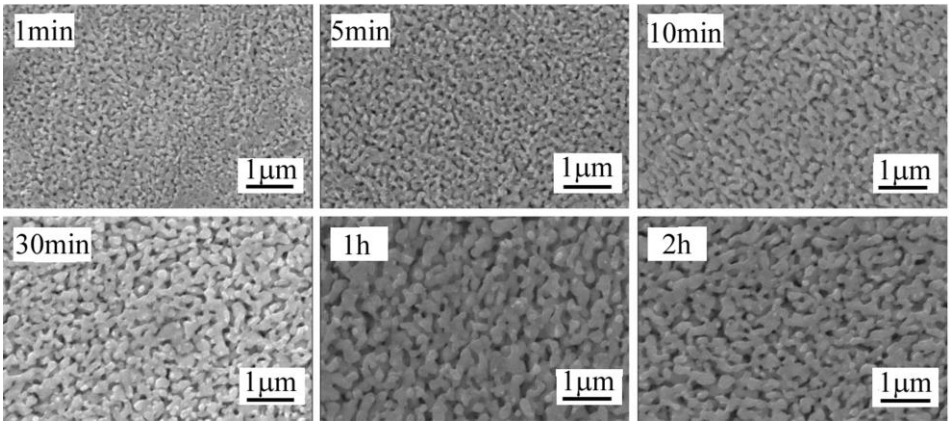

Figure 2. SEM morphology of the nanoporous silver obtained by dealloying $Ag_{22}Zn_{78}$ at 0.4V in 0.1M H_2SO_4 for different time at the temperature of 2°C.

The formation of nanoporous structure process is selective dissolution of zinc atoms and diffusion of silver atoms at alloy/electrolyte interfaces[29,30]. Relationship between the average pore size and dealloying time was plotted in fig.3 (a). Pore size increases with dealloying time which due to the pore structure is on an instability state in thermodynamics. The kinetic data suggests that the coarsening rate of nanopores can be represented by the following formula:

$$d(t)^n = k_0 t \exp(-E/RT) = KtD_s$$

where diffusivity $D_s = D_0 exp(-E/RT)$ and $d(t)$ is pore size at time t ; k_0, K , and D_0 are constants and $k_0 = KD_0$; n is coarsening exponent; R is gas constant; T is the temperature; and E is the activation energy for the nanopore formation and coarsening. The coarsening exponent n can be directly measured by plotting the $ln\ [d(t)]$ vs lnt curves, as showed in Fig. 3(b). The calculated coarsening exponent n for nanoporous silver is 4.19, very close to the kinetic parameter 4. The value n for nanoporous gold is determined to be 3.4-3.7[22], which indirectly shows the rapid diffusion of silver atoms, and the formed pore is commonly larger than gold.

Based on the surface diffusion controlled coarsening mechanism, the diffusivity（Ds）of silver atoms can be estimated by the equation[26]

$$Ds = \frac{[d(t)^4 - d(t_0)^4]kT}{32\gamma t a^4}$$

where k is Boltzmann constant, γ is surface energy, t is the etching time, and a is the lattice parameter. Here, γ =1.302 Jm^{-2}, a =0.409 nm, k =1.3806×10^{-23} J/K, T=275 K， $d(t_0)$=4.046 nm. The surface diffusivity of silver in electrolyte at 2°C is estimated to be 1.2×10^{-16} m^2/s.

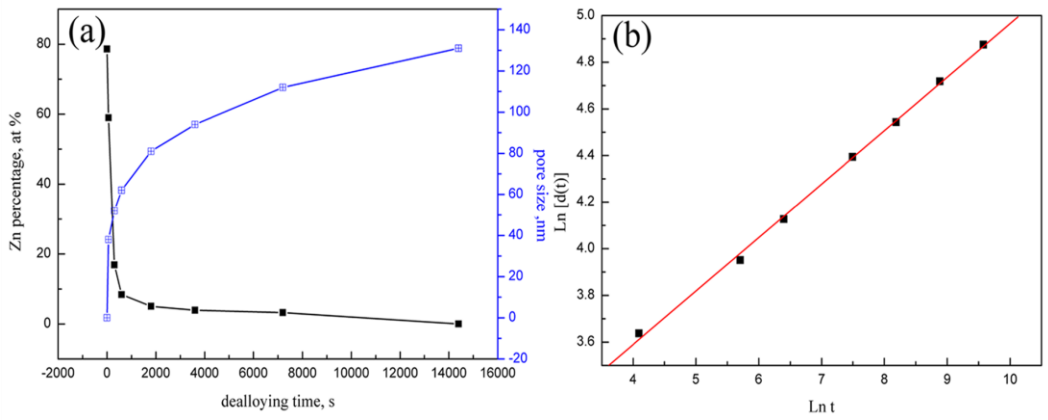

Figure 3. Evolution of the nanopore formation with the dealloying time. (a) Correlation between pore size vs time and Zn composition as a function of dealloying time at temperature 2 °C. (b) Measurment of the coarsening exponent by plotting ln[d(t)] vs ln t.

The composition of the sample that measured by EDX as a function of dealloying time was plotted in Fig.3(a). The majority of zinc atoms dissolved within the first 30 min, during which Zn content decreases to 5 at.pct. At the same time, the pore size increase rapidly. This trend in the evolution of the Zn content is consistent with the results of XRD pattern observation, as showed in Fig.4(a). According to the XRD patterns, $Ag_{22}Zn_{78}$ solid solution only contains ε phases (AgZn3, *hcp*). One minute later of dealloying, the intensities of diffraction peaks of Ag has been emerged, which indicates the nanoporous silver has formed. With increasing the dealloying time, intensities of diffraction peaks of AgZn3 decreases and intensities of diffraction peaks of Ag increases. One hour later, only Ag diffraction peak exists. Additionally, the measured Zn content is in the location that zinc atoms has not been dissolved, so it also reflects thickness of porous silver changing with increasing dealloying time in the electrolyte, which can be described by a linear relation formula according to reference[28].

In summary, the dealloying mechanism has two stages: the initial zinc atoms rapid dissolution (porosity formation stage) and leaching of more zinc from the porous structure as it undergoes ripening by surface diffusion (coarsening stage)[8]. In the first stage, the majority of zinc atoms dissolve and the remaining silver atoms diffuse on the surface to form the initial porosity. This diffusion additionally serves to expose fresh alloy to be attacked and develop bi-continous nanoporous structure. In the next stage, as zinc atoms dissolved, the pore radius increased with high local curvature due to the undercutting of its sidewalls. Interspersed regions exhibiting positive and negative curvatures develop. With positive curvature, the tendency will be for the bonds to stretch, and for negative curvature, the effect of neighboring atoms will be to push the surface atoms in the curved region together. This due to area of fresh alloy surface was diminishing at the same time of the mounds grew, which meant the bases of the mounds were becoming noble element-poor, thus susceptible to undercut. These coupled processes lead to a model in which a pit radius of curvature effectively increased as it penetrated into the bulk. Eventually, the pore radii became greater than $\lambda/2$ (λ expresses spacing of the adjacent ligaments, which is a characteristic parameter relating to the electrolyte, potential, component and so on), a new cluster nucleated, the pit bifurcated, and the process continues ad infinitum and formed the so-called bi-continuous porous structure[31]. Surface chemical instability results in the formation of porosity, which was implemented via competition between surface smoothening and selective dissolution roughening process [32]. It has been acknowledged that during the post-dealloying(coarsening stage), surface diffusion of noble metal element along alloy/solution interfaces plays a key role in the coarsening of nanoporous metals and has a significant influence on the length scales of ligaments[29]. At low temperature, due to the silver atoms diffusivity are suppressed, there are still some un-aggregated silver atoms on the surface when the fresh alloy was attacked by the electrolyte. There will be more un-aggregated silver atoms at alloy/electrolyte interfaces along with the dissolution of zinc atoms, which means they will have more opportunities to nucleate and result in the reduction of λ, generate more pores/ligaments with smaller size.

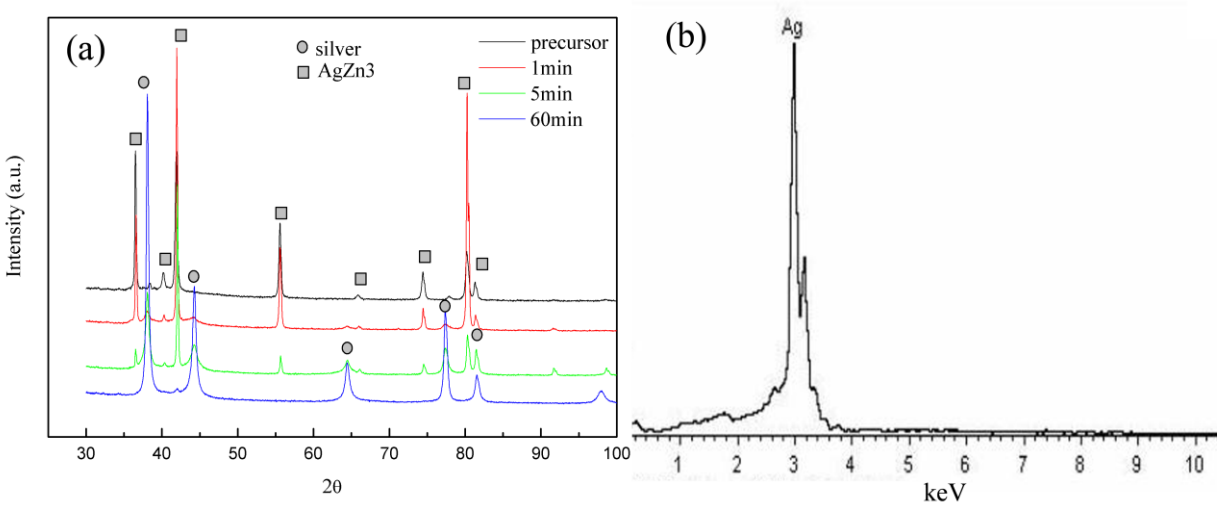

Figure 4. (a) XRD patterns of the alloy before and after dealloying for different time, (b) EDX spectra showing the composition of the sample that dealloyed for one hour.

4. CONCLUSION

Lowering electrolyte temperature can significantly reduce silver atoms surface diffusivity to fabricate finer nanoporous silver with pore range of 38-112nm, far smaller than that fabricated in room temperature by dealloying Ag-Zn. The coarsening exponent of silver at 2 °C in 0.1 M H_2SO_4 is about 4.19 and surface diffusivity of silver atoms are estimated to be 1.2×10^{-16} m^2/s which can explain the pore size of nanoporous silver is commonly bigger than nanoporous gold by dealloying Au-Ag. SEM and EDX observation shows that dealloying process comprises two stages: the initial dissolution and pore formation stage, the latter coarsening stage. XRD patterns show $Ag_{22}Zn_{78}$ solid solution only contains ε phases, with increasing dealloying time, the intensities of diffraction peaks of AgZn3 decreases and intensities of diffraction peaks of Ag increases. AgZn3 phase(hcp) transforms into Ag (fcc) after all the zinc atoms are dissolved.

ACKNOWLEDGEMENT
The authors gratefully acknowledge financial support by the National Science Foundation of China, Higher Education Doctoral Fund of China (20080150002), and Ministry of Education, Liaoning Province government, China (RC-04-15).

References

1. S.H. Joo, S.J. Choi, K.J. Kwa and Z. Liu, *Nature*., 412 (2001) 169.
2. G.C. Bond, D.T. Thompson, *Catal. Rev*., 41 (1999) 319.
3. T. You, O.Niwa, M. Tomita, S. Hirono, *Anal. Chem*., 75 (2003) 2080.
4. Y. Ding, Y.J. Kim, J. Erlebacher, *Adv. Mater*., 16 (2004) 1897.
5. W.B. Liu, S.C. Zhang, N. Li, J.W. Zheng, S.S. An, G.X. Li, *Int. J.Electrochem.Sci*., 7 (2012) 7993.

6. A.Dursun, D.V. Pugh, S.G. Corcoran, *J. Electrochem. Soc*., 150 (2003) B355.
7. H.J. Jin, J. Weissmuller, *Adv.Engi.Mater*., 12 (2010) 714.
8. N.A. Senior and R. C. Newman *Nanotechnology*., 17 (2006) 2311.
9. X. Lu, T.J. Balka, R. Spolenak, E. Arzta, *Thin Solid Films*., 515 (2007) 7122.
10. M. Hakamada, M. Mabuchi, *Mater. Lett*., 62 (2008) 483.
11. Y. Sun, T. John Balk, *Scripta Mater.*, 58 (2008) 727.
12. E. Seker, M.L. Reed, M.R. Begley, *Scripta Mater*., 60 (2009) 435.
13. J. R. Hayes, A.M. Hodge, J.Biener, A.V. Hamza, *J.Mater. Res.*, 21 (2006) 2611.
14. S. Chen, Y.P Chu, J.F Zheng, Z.L Li, *Electrochim Acta*., 54 (2009) 1102.
15. L.S. Su, Y.X. Gan, *Nano Energy*., 1 (2012) 159.
16. D.V. Pugh, A. Dursun, S.G. Corcoran, *J. Mater. Res*., 18 (2003) 216.
17. Z.Q. Li, B.Q. Li, Z.X. Qin, X. Lu, *J. Mater Sci.*, 45 (2010) 6494.
18. C. Zhang, J.Z. Sun, J.L. Xu, *Electrochim. Ac.ta*., 63 (2012) 302.
19. T.T Song, Y.L Gao, Z.H Zhang, *Cryst.Eng.Comm*., 13 (2011) 7058.
20. C.X. Xu, J.X. Su, X.H. Xu, P.P. Liu, H.J. Zhao, F. Tian, Y. Ding, *J. Am. Chem. Soc*., 129 (2007) 42.
21. W.C. Li, T.J. Balk, *Scripta Mater*., 62 (2010) 167.
22. L.H. Qian, M.W. Chen, *Appl. Phys. Lett.*, 91 (2007) 0831051.
23. K. Sieradzki, N. Dimitrov, D. Movrin, C. Mccall, N. Vasiljevic, J. Erlebacher, *J. Electrochem. Soc*., 149 (2002) B370.
24. Y. Ding, M.W. Chen, *MRS Bull*., 34 (2009) 569.
25. J. Weissmuller, R.C. Newman, H.J. Jin, A.M. Hodge, J.W. Kysar, *MRS Bull*., 34 (2009) 577.
26. Z.H. Zhang, Y. Wang, Y.Z. Wang, X.G. Wang, Z. Qi, H. J, C.C. Zhao, *Script Mater*., 62 (2010) 137.
27. A. Dursun, D.V. Pugh, S.G. Corcoran, *J. Electrochem. Soc*., 150 (2003) B355.
28. Z.Q. Li, D.Y Wang, B.Q Li, X. Lu, *J. Electrochem. Soc*., 157 (2010) K223.
29. J. Erlebacher, *J. Electrochem. Soc*., 151 (2004) C614.
30. A.J. Forty, G. Rowlands, *Philos. Mag*. A., 43 (1981) 171.
31. J. Erlebacher, Dekker Encyclopedia of Nanoscience and Nanotechnology DOI:10.1081/E-ENN 120013708, 893.
32. K. Sieradzki, *J. Electrochem. Soc*., 140 (1993) 2868.